

Design Optimization of Switched Reluctance Machines for Maximum Torque/Current Using BEM-Based Sensitivity Analysis

A. Deihimi

Bu-Ali Sina University, Department of Electrical Engineering, Hamedan, Iran
Email: a.deihimi@basu.ac.ir

Abstract—One challenge to predict output performance characteristics of switched reluctance machines (SRM) is the accurate estimation of the minimum inductance of the stator phase at unaligned position of the rotor. In this paper, boundary element method (BEM) is used for this purpose while avoiding time-consuming numerical integrations. So, the method is investigated in terms of accuracy and computational time. Then, to design a SRM with maximum torque per current ratio, a fast optimization method based on sensitivity analysis is presented where BEM is used to evaluate the minimum inductance of the stator phase and a magnetic equivalent circuit is used to estimate the maximum inductance at aligned position of the rotor.

Index Terms—boundary element method, optimization, sensitivity analysis, switched reluctance machine, maximum torque per current ratio

I. INTRODUCTION

During machine design optimization process, machine parameters should be evaluated accurately to determine output performance characteristics for each design candidate. One of the important parameters of a switched reluctance machine (SRM) is the minimum inductance of the stator phase, which affects the area enclosed by electromechanical energy-conversion loop. At unaligned position of the rotor, where the rotor interpolar axis is aligned with the axis of an excited stator pole, the airgap is so large that the computation of the phase inductance would be considered as a linear electromagnetic problem. Due to the complexity of flux paths across the airgap at this position as shown in Fig.1, the accurate value of the inductance is not easy to find. Numerical electromagnetic field analysis methods are often employed to determine the accurate value. But, they are too time-consuming especially for the machine design optimization, where a large number of candidate designs must be evaluated. For example, finite element method (FEM) frequently requires redefining the fine meshes as machine dimension changes. On the other hand, flux tube analysis method as a fast tool assumes that the magnetic field lines follow straight-line segments and circular arcs through certain flux tubes [1-3]. Since the field lines may deflect from the assumed paths, if the shape and number of flux tubes are not properly selected, error will be relatively high [4]. The most desirable approach is one that uses such structures as those of numerical methods, and solves the problem as fast as possible. The algebraic dual energy method (ADEM), as such a method, retains the main body of the FEM. Due to the dual nature, it has much

lower computing-time [5]. This paper shows the usage of boundary element method (BEM) as another method to evaluate the minimum inductance which is more accurate than ADEM with a little tradeoff in computational time. The notable point is a simplification of solution domain considered here so that it requires no numerical integration which is always called as a disadvantage of BEM in terms of computation time. Moreover, this evaluation method is employed in a fast optimization method based on sensitivity analysis to design a SRM with maximum torque per current ratio.

II. COMPUTATION OF MINIMUM INDUCTANCE BY BEM

In comparison with FEM, BEM generally takes more computing-time but needs less element refining to yield more accurate results [6]. The latter may be due to more accurate results obtained on boundary contours, and the former is due to the full coefficient matrix and numerical integrations often faced in the BEM calculations. The numerical integrations can be avoided if simple first-order boundary elements are used where the values of the couple $(A, \partial A/\partial n)$ for all points of the element are the same. To compute the stator phase inductance at unaligned position, the weighted residual method is used to solve the following 2-D Poisson equation for magnetic vector potential (MVP):

$$\nabla^2 A = -\mu_0 J \quad (1)$$

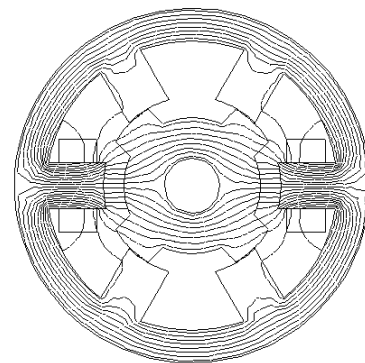


Figure 1. Magnetic flux paths at unaligned position of the rotor

Using Green's second theorem while assuming a fundamental solution to (1) is the weight function, after some manipulations, the final solution for an interior point of i is given by:

$$A_i = \sum_{j=1}^p (G_{ij} \frac{\partial A_j}{\partial n} - H_{ij} A_j) + \mu_0 \frac{J}{2} Q_{ij} \quad (2)$$

$$G_{ij} = \int_{\Gamma_j} w_i d\Gamma \quad (3)$$

$$H_{ij} = \int_{\Gamma_j} \frac{\partial w_i}{\partial n} d\Gamma \quad (4)$$

$$Q_{ij} = \int_{\Gamma_{J,j}} (w_i r \frac{\partial r}{\partial n} - \frac{r^2}{2} \frac{\partial w_i}{\partial n}) d\Gamma \quad (5)$$

Γ and Γ_j are respectively the boundaries of the non-source and source regions. p and q are the numbers of boundary elements for non-source and source regions, respectively. The index of summation j shows different segments of the boundaries of the non-source and source regions. w_i is the fundamental solution to (1) for a solution interior point of i as given by the following:

$$\nabla^2 w_i = -\delta_i \quad (6)$$

$$w_i = \frac{1}{2\pi} \ln\left(\frac{1}{r_i}\right) \quad (7)$$

Using simple first-order boundary elements, the integrations of (3)-(5) will have the following forms which can be readily evaluated analytically.

$$\alpha = \int_{\theta_1}^{\theta_2} \frac{d\theta}{\sigma + \xi\theta + \omega\theta^2} \quad (8)$$

$$\beta = \int_{\theta_1}^{\theta_2} \ln(\sigma + \xi\theta + \omega\theta^2) d\theta \quad (9)$$

θ may be either of Cartesian coordinates (x or y). While solution points are assumed in the middle of first-order boundary elements of the non-source region, either of A or $\partial A/\partial n$ will be known for each element depending upon the type of boundary. This yields the following matrix equation that unknowns (*i.e.* elements of vector $[X]$) are either of A or $\partial A/\partial n$ on each boundary element.

$$[R][X] = [E] \quad (10)$$

After solving the above equation, the minimum phase inductance could be calculated as:

$$L_u = \frac{2N^2}{K.J.S_J} \sum_{k=1}^K A_k \quad (11)$$

N is the number of winding turns, S_J is the area of source region, and k is the index of summation related to

points in the source region. A_k is calculated using (2). Increasing the number of points (K) yields more accurate values.

III. COMPUTATION OF MINIMUM INDUCTANCE BY ADEM

ADEM uses lower energy bound (LEB) and upper energy bound (UEB) to determine the average stored magnetic energy for each phase of SRM [5]. For a constant phase current of I the inductance is given by:

$$L = 2W/I^2 \quad (12)$$

The stored energy (W) is given by the following volume integrations:

$$W = \frac{1}{2} \int_V \mathbf{B} \cdot \mathbf{H} dV = \frac{1}{2} \int_V \mathbf{J} \cdot \mathbf{A} dV \quad (13)$$

The lower and upper bounds of the inductance are calculated from (12) using LEB and UEB, respectively.

The minimum phase inductance is given by:

$$L_u = \frac{2W_{ave}}{I^2} = \frac{2}{I^2} \left[\left(\int_V \mathbf{J} \cdot \mathbf{A}_L dV - \frac{1}{2} \int_V \mathbf{B}_L \cdot \mathbf{H}_L dV \right) + \left(\frac{1}{2} \int_V \mathbf{B}_U \cdot \mathbf{H}_U dV \right) \right] \quad (14)$$

The expression in the first parenthesis is the LEB, and that of the second one is the UEB. The LEB is obtained by approximating the magnetic vector potential (MVP) as a polynomial in x and y , while forced to satisfy only Gauss' law and Dirichlet boundary conditions. The UEB is obtained by approximating the magnetic field intensity (MFI) as a vector-polynomial in x and y , while forced to satisfy only Ampere's law and Neumann boundary conditions. Therefore, the inductance is obtained from average stored magnetic energy, *i.e.* $W_{ave} = (LEB + UEB)/2$. The energy bounds can be improved towards the actual value by increasing the order of polynomial approximations (or the number of free coefficients of polynomials) for MVP and MFI. In order to have an equidistance error condition, *i.e.* the same error for two energy bound and hence little error in W_{ave} , the number of free coefficients of each energy bounds should be selected properly. In [5] an approximate method has been proposed to find the proper number of free coefficients of polynomials in both energy bounds so that the errors cancel each other out during computation of W_{ave} . It is assumed that the error function of each energy bound versus the number of free coefficients of M is a straight-line in a log-log plot as:

$$E = K_1 M^{(K_2)} \quad (15)$$

K_1 and K_2 are constants that should be determined by using at least three values of the energy bound. If the error for either of energy bounds is known, the equidistance error condition will be imposed to the error of another bound by finding K_1 , K_2 and M using (15).

IV. RESULTS AND COMPARISON OF BEM AND ADEM

The SRM geometry at unaligned position is cast in Cartesian coordinates. The simplified geometry of the airgap at this position shown in Fig. 2 can play an important role in the simplicity and speedy of the design optimization of SRM based on sensitivity analysis that will be discussed later. The end core effects are also ignored. This is only true for machines with a relatively high ratio of stator axial length to rotor diameter. Assuming a high permeability for iron cores, the solution region is restricted to airgap region as shown in Fig. 2.

To evaluate the minimum phase inductance using the ADEM, the non-source region is subdivided to only one region for computing LEB, and to 6 subregions for the for computing UEB, following stages like FEM. The number of free coefficients selected for each of energy bounds determines the accuracy of the calculated inductance. Table I shows the calculated results of LEB, UEB, and their errors with respect to the actual value of the stored energy for different number of free coefficients for a SRM of geometry given in Table II.

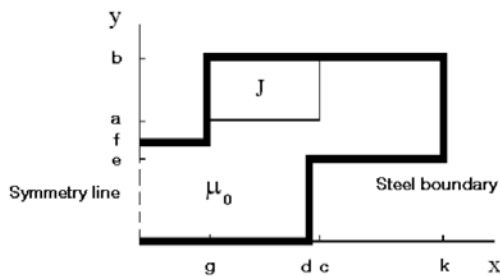


Figure 2. Simplified air-gap model at unaligned position

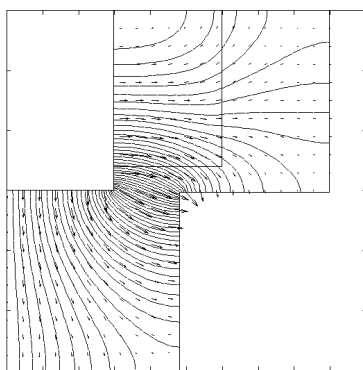


Figure 3. Airgap flux contours obtained from solution by FEM

TABLE I.
CALCULATED RESULTS OF ENERGY BOUNDS USING ADEM FOR THE GIVEN SRM

Lower energy bound			
<i>M</i>	LEB value (J/m)	Error (%)	<i>M</i> -UEB for equidistance error from (10)
1	0.030074	85.36	3.6
3	0.06967	66.10	4.08
6	0.089429	56.48	4.4057
10	0.1	51.34	4.6156
15	0.1122	45.40	6.9
21	0.1157	43.70	6.993
Upper energy bound			
<i>M</i>	UEB value (J/m)	Error (%)	<i>M</i> -LEB for equidistance error from (10)
2	0.489	137.96	0.9052
6	0.3084	50.07	5.2
12	0.225	9.49	91.63
20	0.212	3.16	610.8
30	0.210	2.19	1149.7

TABLE II.
THE GEOMETRY OF THE EXEMPLAR SRM

Parameter	Value (cm)	Parameter	Value (cm)
a	3.40	e	2.97
b	6.00	f	3.00
c	3.00	g	1.49
d	2.40	k	4.50

TABLE III.
CALCULATED RESULTS OF ENERGY USING BEM FOR THE GIVEN SRM

No. of boundary elements	Energy (J/m)	Error (%)
8	0.065853	67.95
16	0.1943	5.45
24	0.202	1.7
32	0.204	0.73
40	0.205	0.24

TABLE IV.
COMPARISON OF TWO METHODS

Method	Computing time (%)	Error (%)
ADEM	100 (=base)	0.293
BEM	114.6	0.24

The actual value of the stored energy which was evaluated by FEM (refer to Fig. 3) is 0.2055 J/m. Although UEB converges much faster than LEB by increasing the number of free coefficients, it requires a large value of the number of free coefficients to reach the accurate result. In the last column of Table I, the number of free coefficients of another energy bound to make equidistance error condition is given. As seen, they are not equal to any integer number being proper for approximations used. Therefore, there is always some error. Table III gives the results of the stored magnetic energy estimated by the BEM for different number of boundary elements for the same SRM geometry given in Table II. The number of boundary elements more than 32 yields errors less than %1. Evidently, BEM converges fast by increasing the number of boundary elements.

Table IV shows a comparison of methods in terms of computation speed and error. In order to have minimum error for ADEM, the number of free coefficients is selected 12 for UEB and 91 for LEB. The number of boundary elements for BEM is 40. As seen, although BEM takes more time, it results in more accurate estimation.

V. SRM DESIGN OPTIMIZATION BASED ON SENSITIVITY ANALYSIS

The torque produced by a single phase in a SRM is generally computed from the concept of coenergy as the following:

$$T(i, \theta) = \frac{\partial W'(i, \theta)}{\partial \theta} = \frac{\partial}{\partial \theta} \int_0^i \lambda(i, \theta) di \quad (16)$$

The amount of the phase torque depends upon the area enclosed in the energy conversion loop, *i.e.* the trajectory of λ - i . Such an energy conversion loop is shown in Fig. 4. In special case, a SRM with no saturation and excited by a flat-topped phase current, *i.e.* with a constant phase current of I during the whole phase conduction angle, has the output phase torque given by:

$$T = \frac{I^2}{2} \frac{\partial L}{\partial \theta} = \frac{I^2}{2\beta_s} (L_m - L_u) \quad (17)$$

L_m is the maximum phase inductance at aligned position, and β_s is the stator pole arc. Fig. 5 illustrates inductance and phase current shapes in this case.

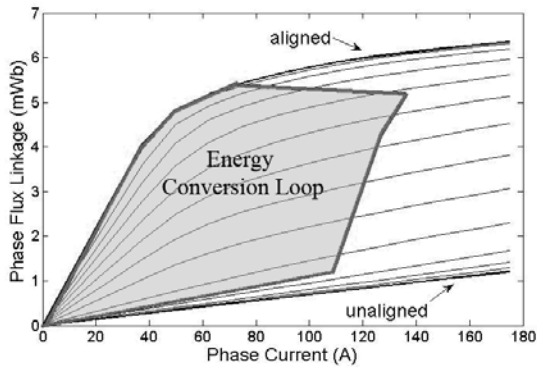


Figure 4. Magnetization characteristics and energy-conversion loop

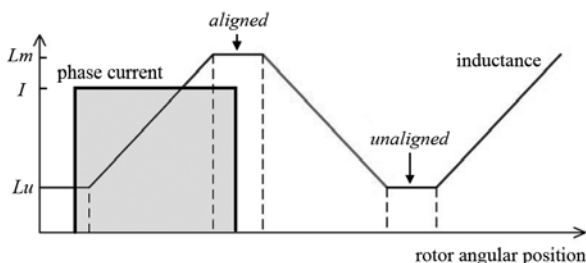


Figure 5. Airgap flux contours obtained from solution by FEM

As a result, simultaneous maximization of the difference of $(L_m - L_u)$ and minimization of the stator

pole arc β_s will maximize T/I^2 that could be considered as an appropriate index to produce a high torque using a low phase current. In case of saturation, if the phase current is flat-topped or close it, the simultaneous maximization of $(L_m - L_u)$ and minimization of β_s will be also in the direction of obtaining a high torque from a low phase current. Because they increase the area between aligned and unaligned magnetization curves (Fig. 4) and in turn increase the available area of energy conversion loop. In practice, there is always an attempt to operate the SRM with a flat topped phase current by controlling and forming the phase excitation. On the other hand, since the whole area between aligned and unaligned magnetization curves should be enlarged to maximize energy conversion loop, the different levels of current magnitude (I) have to be taken into account for optimization problem. Evidently, this considers all saturation effects in the aligned magnetization curve. Therefore, the optimization problem is defined as:

$$\max F = (1/\beta_s) \left[\frac{1}{N} \sum_{n=1}^N L_m(I_n) \right] - L_u \quad (18)$$

over all parameters of machine
subject to constraints on parameters and outputs

N is the total number of current levels to cover both non-saturated and saturated regions on aligned magnetization curve. The minimum inductance in (18) which has the same value for all practical current levels is to be computed by BEM discussed in section II using a simplified airgap domain at unaligned rotor position shown in Fig. 2. The maximum inductance is to be calculated for each current level using a simple nonlinear magnetic equivalent circuit composed of lumped permeance elements [1-3]. A sensitivity analysis is used to solve the optimization problem in (18). The sensitivity is given as the total derivative of the objective function (F) with respect to each design parameter of the machine. It reveals the direction of changes in each parameter at each incremental step so that the objective function moves gradually to the maximum value. The sensitivity of the objective function with respect to the i -th design parameter of P_i is given by:

$$S_i = \frac{\partial F}{\partial P_i} = \Delta_{\beta_s} + (1/\beta_s) \left[\frac{1}{N} \sum_{n=1}^N \frac{\partial L_m(I_n)}{\partial P_i} \right] - \frac{\partial L_u}{\partial P_i} \quad (19)$$

Δ_{β_s} is zero for all design parameters except for $P_i = \beta_s$ which is given by:

$$\Delta_{\beta_s} = (-1/\beta_s^2) \left[\frac{1}{N} \sum_{n=1}^N L_m(I_n) \right] - L_u \quad (20)$$

It is required to calculate sensitivities of L_m and L_u with respect to design parameters. The sensitivity of L_u evaluated using BEM and based on (11) is:

$$\frac{dL_u}{dP_i} = \frac{2N^2}{K.J.S_j} \sum_{k=1}^K \left(\frac{\partial A_k}{\partial P_i} + \frac{\partial A_k}{\partial [X]} \cdot \frac{d[X]}{dP_i} \right) \quad (21)$$

The derivative $\partial A_k / \partial P_i$ is evaluated by differentiating both sides of (2) with respect to P_i . The derivative $d[X] / dP_i$ is obtained by solving the following equation, which results from differentiating the both sides of (10) with respect to P_i [7].

$$[R] \cdot \frac{d[X]}{dP_i} = \frac{d[E]}{dP_i} - \frac{d[R]}{dP_i} \cdot [X'] \quad (22)$$

Prime represents the values at previous step. The derivatives $d[R] / dP_i$ and $d[E] / dP_i$ in (22) are obtained from boundary integrations calculated analytically before. The derivative $\partial A_k / \partial [X]$ in (21) is a simple column matrix with zero and one as elements. The sensitivity of L_m with respect to P_i is derived from a magnetic equivalent circuit of the SRM at aligned position:

$$\frac{\partial L_m}{\partial P_i} = \frac{\partial}{\partial P_i} (N^2 \Lambda_{eq}) \quad (23)$$

Λ_{eq} is the equivalent magnetic permeance seen by the MMF produced by the phase winding. Since the magnetic circuit is nonlinear, a discrete differentiation is preferred. A steepest decent method is used as an optimization algorithm. Recent values of design parameters at each step are obtained from last values at previous step:

$$\mathbf{P}^{(n+1)} = \mathbf{P}^{(n)} + \lambda \mathbf{S}^{(n)} \quad (24)$$

$\mathbf{P}^{(n+1)}$ and $\mathbf{P}^{(n)}$ denote vectors of design parameters at n th and $(n+1)$ th iteration step, respectively. \mathbf{S} is a vector of the sensitivity of the objective function with respect to design parameters, and λ is the step size. The above algorithm is applied for design optimization of a 12/8 four-phase 35 kW SRM. A prototype constructed and reported in [8] is selected for comparison. The values of the important parameters of the prototype are given in Table V. Also, the results of design optimization for a similar SRM are given where the variables for design are rotor pole arc, rotor yoke width and rotor diameter, while other parameters are invariable and the same as those of the prototype. A comparison of peak values of static torque profiles for different levels of the phase current given in Table VI shows the effectiveness of the optimization method.

V. CONCLUSIONS

The paper shows beneficial features of BEM for computation of the minimum inductance of SRMs while using a simplified airgap domain cast in Cartesian coordinates at unaligned position.

TABLE V.
VALUES OF PARAMETERS FOR PROTOTYPE SRM AND OPTIMUM DESIGN

Parameter	Prototype	Optimum design
Stator outer diameter (mm)	215	215
Stator yoke width (mm)	20	20
Rotor yoke width (mm)	52	46.3
Rotor diameter (mm)	146	139.4
No. of winding turns	18	18
Rotor pole arc (degree)	18	17.7
Stator pole arc (degree)	13	13

TABLE VI.
COMPARISON OF MAXIMUM STATIC TORQUES AT DIFFERENT PHASE CURRENT LEVELS FOR PROTOTYPE SRM AND OPTIMUM DESIGN

Current level (A)	Max. static torque (Nm) Prototype	Max. static torque (Nm) Optimum Design
5	7.5	11.2
15	28.1	33.3
25	60.7	62.5
35	110.5	115.1

Forty boundary elements results in sufficient accuracy and speed. Also, a sensitivity analysis for SRM design optimization is employed to maximize torque/current while using BEM to estimate minimum inductance and a magnetic equivalent circuit to evaluate maximum inductance. A comparison between a prototype and resulting optimum design shows effectiveness of the method.

REFERENCES

- [1] A. Deihimi, S. Farhangi, G. Henneberger, "A general nonlinear model of switched reluctance motor with mutual coupling and multiphase excitation," *Electrical Engineering*, Vol. 84, No. 3, pp. 143-158, July 2002.
- [2] A. Deihimi, "Improved model of saturated regions in magnetic equivalent circuits of highly saturated electromagnetic devices," *11th International Conference on Optimization of Electrical and Electronic Equipment, OPTIM 2008*, Brasov, pp. 45-50, Romania, 2008.
- [3] Corda, and J. M. Stephenson, "Analytical estimation of the minimum inductances of double salient motor," *Int. Conf. on Stepping Motors and Systems*, pp. 50-59, Sept. 1979.
- [4] D. P. Tormey, D. A. Torrey, and P. L. Levin, "Minimum airgap-permeance data for the doubly-slotted pole structures common in variable-reluctance-motors," *IEEE IAS Annual Meeting*, pp. 196-200, 1990.
- [5] M. Tolikas, J. H. Lang, and J. L. Kirtley, "Algebraic dual-energy magnetic analysis with application to variable reluctance motor design," *IEEE IAS Annual Meeting*, pp. 412-418, 1995.
- [6] C. Brebbia, *Boundary Element Method for Engineers*, Pentech Press, London, 1980.
- [7] C. S. Koh, S. Y. Hahn, T. K. Chung, and H. K. Jung, "A sensitivity analysis using boundary element method for shape optimization of electromagnetic devices," *IEEE Tran. Magn.*, Vol. 28, No. 2, pp. 1577-1580, March 1992.
- [8] S. Risse and G. Henneberger, "Design and optimization of a switched reluctance motor for electric vehicle propulsion," *International Conference on Electrical Machines (ICEM 2000)*, Espoo, Finland, pp. 1526-1530, 2000.